http://dx.doi.org/10.21577/0100-4042.20170801 *Quim. Nova,* Vol. 45, No. 1, 48-52, 2022

Artigo

A NOVEL FLUORESCENCE SENSOR FOR THE DETECTION OF CHLORIDE ION IN ARTIFICIAL SWEAT AND ENVIRONMENTAL WATER WITH NITROGEN-DOPED GRAPHENE QUANTUM DOTS

Xuemei Fan[a,b,c,*], Shumin Wang[b], Zhejian Li[b], Ping Liu[b], Yimeng Wang[b], Qiangqiang Sun[b], Lingmin Yu[a] and Xinhui Fan[a,b]
[a]School of Materials science and Chemical Engineering, Xi'an Technological University, Xi'an, 710021, China
[b]College of Chemical Engineering and Modern Materials, Shangluo University, Shangluo, 726000, China
[c]Research Centre of Graphene Technology and Application, Shangluo University, Shangluo, 72600, China

Recebido em 08/04/2021; aceito em 12/07/2021; publicado na web em 03/08/2021

A new fluorescent detection route for chloride ion was designed with Nitrogen-doped graphene quantum dots (N-GQDs), which were prepared by a traditional hydrothermal method with citric acid as carbon source and urea as nitrogen source. The prepared N-GQDs solution was light yellow, and the freeze-dried solid was black. It emitted blue light under ultraviolet light. Meanwhile, The N-GQDs were characterized by TEM, XRD, UV-Vis and fluorescence, the results indicated that the N-GQDs had good dispersibility, photostability and excitation independent emission fluorescence. After addition of Ag^+ solution, Ag^+ combined to the surface functional groups of N-GQDs, resulting in an obvious quenching of the fluorescence intensity of N-GQDs. Nevertheless, the fluorescence intensity recovered significantly with the addition of Cl^- to the N-GQDs/Ag^+ system, this was because of AgCl was formed due to the "soft hard acid base principle". The change of fluorescence intensity had a linear response to the chloride ion concentration in the range of 8.5-300 μmol L^{-1}, with a detection limit (LOD) of 0.1 μmol L^{-1}. To authenticate the application, the proposed method has been successfully used for quantitative analysis of chloride ion in real samples, including artificial sweat and environmental water.

Keywords: nitrogen-doped graphene quantum dots; chloride ion; fluorescence.

INTRODUCTION

Chloride ion (Cl^-) is one of the most common anion, which is indispensable for disinfection in environmental water and is extensively used in many production processes.[1] The excess Cl^- would easily accelerate corrosion reaction of industrial equipment, inhibit crop growth and lead to soil acidification and salinization.[2] In addition, the salt content of canned foods exceeding the recommended salt limit is harmful to human health.[3] In particular, the monitoring of Cl^- in serum, urine and sweat is essential for the diagnosis of many diseases, including fatal Cystic Fibrosis.[4] Therefore, a fast and accurate method for Cl^- detection is necessary.

Several techniques including titration,[5] colorimetry,[6,7] mass spectrometry,[8] ion chromatography[9-11] and electrochemistry,[12-15] have been applied for the detection of Cl^-. Fluorescence is a powerful technology due to its salient advantage such as simple, reliable, economic and high sensitive. In recent years, a number of fluorescent materials such as Ag^+-benzimidazole complexes,[16] lucigenin-doped silica nanoparticles,[17] Ag-modified porous g-C_3N_4 nanosheets[18] and BeQ1 and BeQ2[19] have been reported for the detection of Cl^-.

Graphene quantum dots (GQDs), a late-model zero-dimensional (0D) luminescent nanomaterials of the graphene family with a size of less than 10 nm,[20] have been widely used for their unique characteristics of good electronics, good water-solubility and excellent biocompatibility, as well as non-toxicity and strong photoluminescence.[21] As a new type of quantum dots, GQDs have superior optical and electrical properties over the traditional semiconductor quantum dots owing to their quantum confinement and edge effects.[22] Nevertheless, the application of GQDs in fluorescent probes has been limited for its non-specificity and low quantum yield.[23] So, some heteroatom such as *N*, *S*, *B* and *P* have been doped into GQDs to improve the optical properties of GQDs.[24-27]

In this study, we reported a new label-free fluorescent sensor for fast detection of Cl^- based on N-GQDs. As illustrated in Scheme 1A, N-GQDs were prepared by a traditional hydrothermal method with citric acid as carbon source and urea as nitrogen source. Ag^+ had a good affinity for oxygen groups and amino groups on the surface of N-GQDs, forming N-GQDs/Ag^+ complexes, which resulted in an obvious quenching of the fluorescence signal of N-GQDs. When Cl^- was added to the N-GQDs/Ag^+ system, the fluorescence signal recovered which was due to AgCl were formed for the strong interaction between Ag^+ and Cl^- (Scheme 1B). The increase value of fluorescence signal was proportional to the concentration of Cl^-. Therefore, a fluorescent sensor for detection of Cl^- was established. This label-free optical sensor was simple and applied in accurate detection of Cl^- in artificial sweat and environmental water successfully.

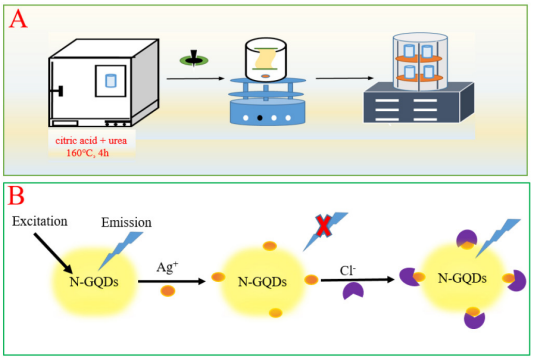

Scheme 1. *Schematic illustration showing the preparation process of N-GQDs (A), the principle of Cl^- assay based on N-GQDs (B)*

EXPERIMENTAL

Materials and instrumentation

Citric acid (CA) and urea were obtained from Aladdin Reagent Company. Silver nitrate ($AgNO_3$), dihydrate sodium phosphate

*e-mail: fanxuemei527@163.com

monobasic dehydrate ($NaH_2PO_4 \cdot 2H_2O$) and sodium phosphate dibasic dodecahydrate ($Na_2HPO_4 \cdot 12H_2O$) were purchased from Sinopharm Chemical Reagent Co., Ltd (Shanghai, China). All the reagents are analytical grade and all the working solutions were prepared with ultrapure water (> 18.2 MΩ cm^{-1}) supplied by a Milli-Q Lab system.

LC-10N-50A vacuum freeze dryer was used to freeze-dry the prepared N-GQDs solution (Shanghai lichen Bangxi Instrument Technology Co., Ltd). The morphology and size of the N-GQDs were obtained by the JEM-2100 transmission electron microscopy (JEOL, Japan). X-ray diffraction (XRD) was conducted by PANalytical Xpert Pro (Almelo, Netherlands) in the 2θ range of 10-80° with a step size 0.01° using Cu Kα (λ = 0.154 nm) radiation. The Ultraviolet-visible (UV-vis) absorption spectrum was recorded on a UV-vis spectrometer (UV-2450). The fluorescence spectra was performed by a F-4600 spectrofluorometer (Hitachi, Japan).

Synthesis of N-GQDs

N-GQDs were synthesized using a hydrothermal method following the procedure described by Chen *et al.*[28] 0.21g CA and 0.18 g urea were dissolved in a beaker with 25 mL ultrapure water, then heated in a hydrothermal reactor at 160 °C for 4 h. The prepared product was filtered with a filter membrane of 0.22 μm and dialyzed with a dialysis bag (retaining molecular weight of 1000 Da) for 3 days to remove impurities. The obtained solution was freeze-dried to obtain the solid, and then N-GQDS with an accurate concentration of 0.1 mg mL^{-1} was prepared.

Measurement procedure for Cl^-

For Cl^- detection, 100 μL N-GQDs (0.1 mg mL^{-1}), 100 μL Ag^+ (1.0×10^{-5} mol L^{-1}) and 200 μL PB buffer (0.01 mol L^{-1}, pH 7.0) were mixed for 20 min. Afterwards, Cl^- solution of different concentration was added to the mixture and reacted for 25 min. The fluorescence emission spectra were documented at 450 nm under the excitation at 360 nm and Cl^- was quantitative by the fluorescence enhancement intensity $\Delta F = F\text{-}F_0$, where F_0 and F represented the fluorescence intensities of the N-GQDs in the presence and absence of Cl^-, respectively.

RESULTS AND DISCUSSION

Characterization of NGQDs

Figure 1A and Figure 1B showed the transmission electron microscopy (TEM) image and size distributions of the N-GQDs, it revealed that the produced N-GQDs were spherical with size distribution ranging from 1.5 nm to 5.4 nm. The inset of Figure 1A displayed that the synthesized N-GQDs solution was light yellow, and the freeze-dried solid was black. Figure 1C was the XRD pattern of N-GQDs, the result illustrated that there was a single peak near 2θ = 24° of (002) crystal plane, which indicated the formation of GQDs structure.[29] As can be seen from Figure 1D, the UV-Vis absorption spectra of N-GQDs exhibited a maximum absorption wavelength of 340 nm, this was just the n-π* transition of C=O and C–N functional groups.[30] The inset of Figure 1D showed that the aqueous solution of N-GQDs glowed bright blue light when illuminated by an ultraviolet lamp. As depicted in Figure 1E, the maximum fluorescence emission peak of N-GQDs was at 450 nm with the excitation wavelength at 368 nm, which was consistent with the results reported in the previous literature.[21] Moreover, as shown in Figure 1F, the emission wavelength of N-GQDs almost unchanged when the excitation wavelength changed in the range of 335-360 nm, this excitation independence indicated that the size and surface state of N-GQDs were consistent.[31]

Feasibility for Cl^- assay

The feasibility for Cl^- determination using N-GQD as a fluorescence probe was discussed and the results were exhibited in Figure 2. It was shown that the fluorescence signal of N-GQDs at 450 nm can be quenched by Ag^+, and while adding Cl^- to the N-GQDs/Ag^+ system, the fluorescence signal was restored to about 91.8% of the original, which demonstrated that our method for Cl^- was feasible. The process can be interpreted that Ag^+ can form N-GQDs/Ag^+ complexes with N-GQDs resulting a quenching of the fluorescence of N-GQDs. In addition, when the Cl^- was present, AgCl was further generation for the strong interaction between Ag^+ and Cl^-, so a recover of fluorescence signal was acquired.

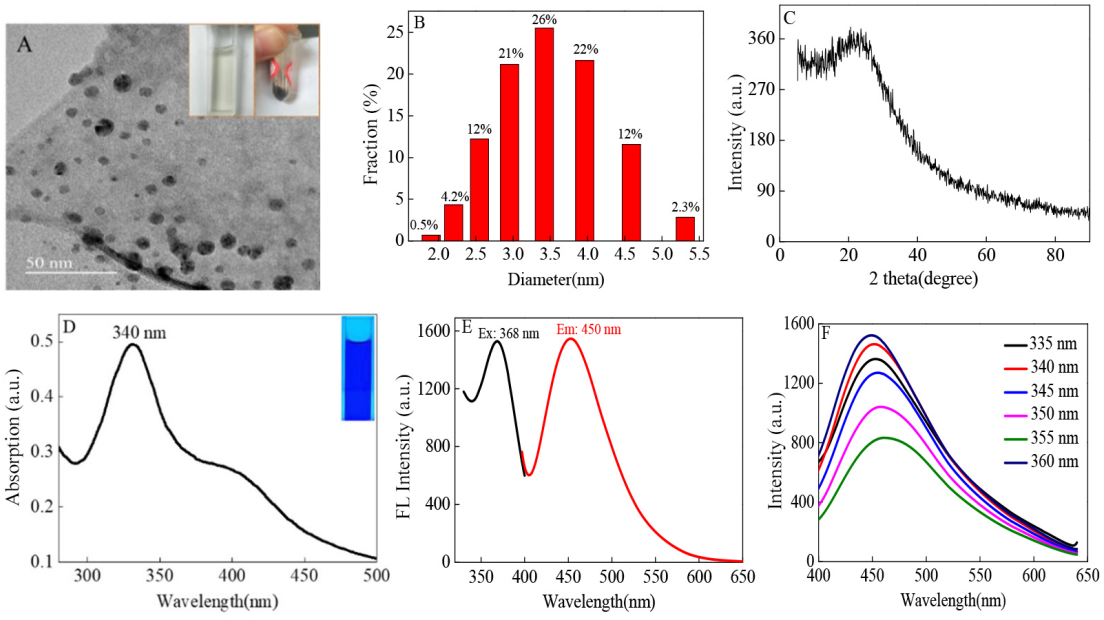

Figure 1. *TEM image (A, inset were photos of N-GQDs), size distributions (B), XRD pattern (C), UV-Vis spectra (D, inset was photo of N-GQDs illuminated by an ultraviolet lamp) and fluorescence spectra (E) of NGQDs; Fluorescence spectra at different excitation wavelengths (F)*

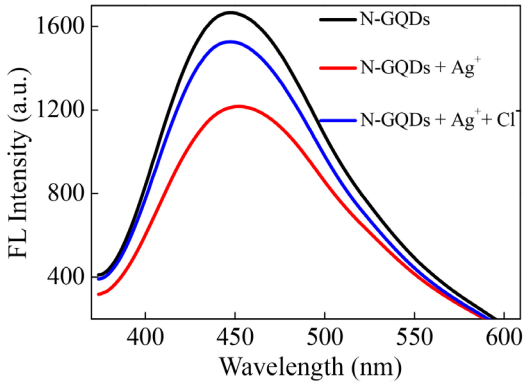

Figure 2. *The feasibility for Cl⁻ assay*

Fluorescence response strategy for Cl⁻ determination

The detection performance was elevated by optimizing the experimental conditions, including the concentration and the reaction time of Ag^+, pH and action time of Cl^-, respectively. First of all, the reaction time of Ag^+ with N-GQDs had an effect on the detection of Cl^-. Figure 3A displayed that as the reaction time increased, the ΔF gradually increased and appeared a platform at 20 min, this indicated that Cl^- indeed reacted with Ag^+ which coming from N-GQDs/Ag^+ and the fluorescence was recovery. At the same time, it still declared that Cl^- can react with all of Ag^+ successfully at 20 min. Hence, the reaction time for Ag^+ was set at 20 min. In addition, the influence of Ag^+ concentration was investigated specifically. It was easy to think that as the increases of the amount of Ag^+ content, more N-GQDs/Ag^+ will be formed, when adding Cl^-, more fluorescence signal will be recovery. Figure 3B just confirmed this conclusion (ΔF increased as the amount of Ag^+), it also indicated ΔF reached maximum at 1.0 × 10^{-5} mol L^{-1}. Therefore, 1.0 × 10^{-5} mol L^{-1} of Ag^+ was selected. The react time of the fluorescence sensor with Cl^- was researched and the result displayed in Figure 3C. For 250 μmol L^{-1} Cl^-, when the react time increased from 5 to 30 min, fluorescence intensity became stable after 25 min, which meant that 25 min can achieve equilibrium. So, the action time of the sensor with Cl^- was set at 25 min. As illustrated in Figure 3D, with increasing the pH in the range of 5.8 to 7.8, ΔF gradually increased and reached maximum at pH of 7.0. This was because the amino groups on the surfaces of the N-GQDs were protonated at lower pH and the coordination degree of Ag^+ with amino groups was responsively reduced, thereby Cl^- can only take a small amount of Ag^+ in Ag^+/N-GQD, less fluorescence was recovery. Whereas, when the pH became higher than 7.0, Ag^+ may hydrolyze and combine with OH^- to form AgOH, which was instability and became to Ag_2O. This lead to the interaction between Ag^+ and Cl^- decreases and less fluorescence was recovery. Therefore, the pH 7.0 was chosen in the future.

Detection of Cl⁻ using N-GQDs as fluorescent probe

Under the optimal detection conditions, a quantitative detection of Cl^- was performed. As shown in Figure 4A, with the concentration of Cl^- increase, gradually enhancement of fluorescence intensity was observed. Notably, a good linear relationship was existed between the enhancement of the fluorescence value and the concentration of Cl^- ranging from 8.5 to 300 μmol L^{-1}. The linear regression equation was $F\text{-}F_0 = 1.0868\ C + 19.4801$ where C was the concentration of Cl^- (Figure 4B). The correlation coefficient was 0.9899. At the same time, the detection limit was calculated to be 0.1 μmol L^{-1} at a signal-to-noise ratio of 3 (S/N = 3). We compared our proposed sensor with other methods for Cl^- detection. As illustrated in Table 1, though the linear range was not the widest among these sensors, it was wider than those reported by Lima,[7] Bujes-Garrido,[13] Bujes-Garrido[15] and Xiao,[17] it was obvious that the detection limit was better than most of the reported literatures except Yakoh's, [6] Lima's[7] and Wan's work.[14]

In addition, for real application, interference species may effect on the response of Cl^-. So, some relatively important cations and anions interfering species such as Na^+, K^+, Ni^{2+}, Mg^{2+}, NO_3^-, HCO_3^- and SCN^- were carried out to evaluate the selectivity for detection of Cl^-, respectively. As can be seen in Figure 5A, after adding different ions

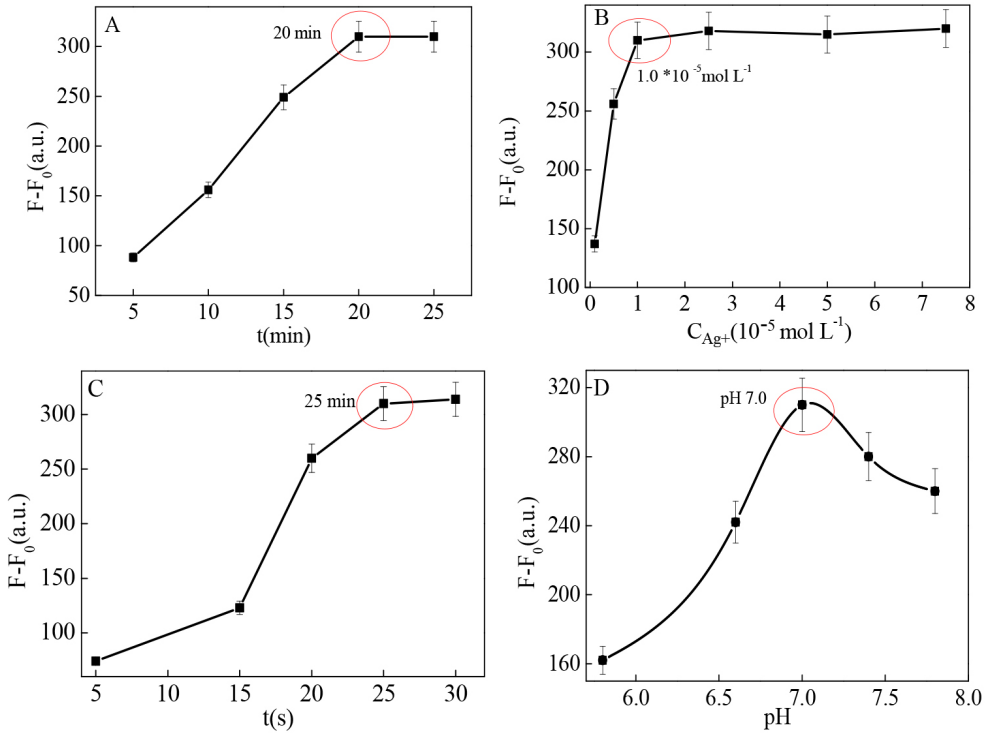

Figure 3. *Effect of reaction time (A) and concentration of Ag^+ (B), action time of Cl^- (C) and pH (D) on the fluorescence intensity for the detection of Cl^-*

in N-GQDs/Ag^+ system, it seemed that no significant fluorescence recovery of other ions obtained except for Cl^-, demonstrating the binding ability of these ions with Ag^+ was weaker than that of with Cl^-, this can cause unconspicuous fluorescence recover after addition the interfering substance. Furthermore, Figure 5A also depicted that the fluorescence recovery was not obvious when all the above-mentioned common cations and anions co-existed in the NGQDs/Ag^+ system. In conclusion, all of the above conclusions can indicate that this method had good selectivity in the detection of Cl^-.

Meanwhile, to investigate the stability for detection of Cl^-, 80 μmol L^{-1} of Cl^- was measured continuously in seven days and the results were shown in Figure 5B, revealing a relative RSD (Relative standard deviation) of 5.09%, this indicated good stability for detection of Cl^- in N-GQDs/Ag^+ system.

Application in real samples

In order to assess the application reliability of the method provided, the real water sample obtained from the ShangLuo DanJiang (ShaanXi, China) were quantitatively analyzed (Table 2). The water sample was diluted for double times by 0.01 mol L^{-1} PB (pH 7.0) without any pretreatment. The content of Cl^- in real water was not detected, so the standard addition method was carried out to evaluate the reliability of the sensor. Different concentrations of Cl^- was added to water sample in the linear range and the fluorescent responses were measured according to the experimental method. The recoveries were between 97.4% and 103.6%.

Furthermore, the level of Cl^- in sweat is a recognized biomarker for the genetic disorder cystic fibrosis. Therefore, the accurate quantitation of Cl^- in sweat is an important tool in the diagnosis of this deadly disease. Three artificial sweat samples with different concentrations of Cl^- (20 mmol L^{-1}, 50 mmol L^{-1} and 80 mmol L^{-1}) were prepared according to the British Standard (BS EN1811-1999), while diluted for 1000 times and act as the analysis samples. The recovery rate was estimated by standard addition method (Table 3). The recoveries ranged from 96.5 to 104.8% with the RSD (relative standard deviation) of 2.3 to 3.9% (Table 3). These results indicated that N-GQDs/Ag^+ system can be used for the determination of Cl^- in artificial sweat samples, and it had good potential in the detection and diagnosis of cystic fibrosis.

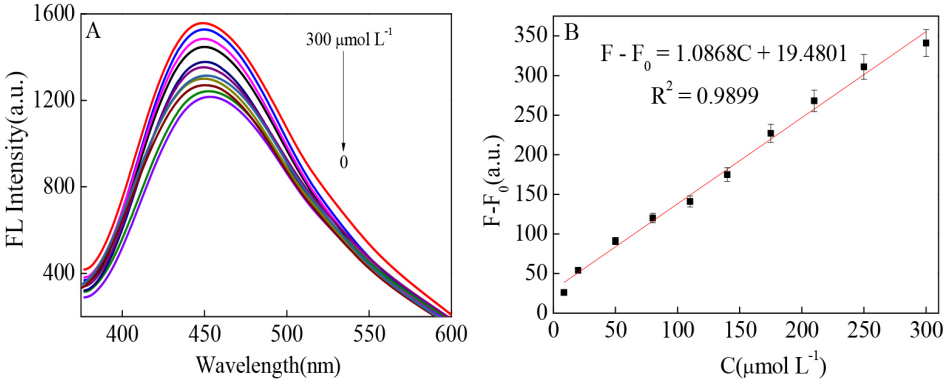

Figure 4. *Fluorescence spectra of Ag^+/N-GQD under various concentrations of Cl^-, from bottom to top: 0, 8.5, 20, 50, 80, 110, 140, 175, 210, 250 and 300 μmol L^{-1}, respectively (A), Calibration curve of Cl^- (B)*

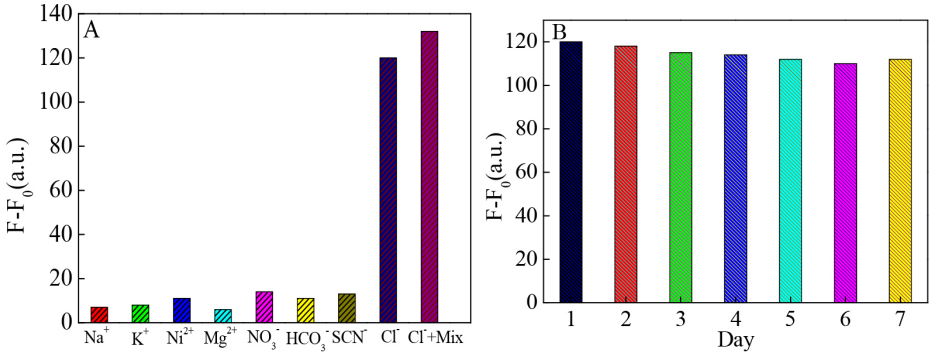

Figure 5. *Selectivity (A) and stability (B) for detection of Cl^- in N-GQDs/Ag^+ system. Cl^-: 80 μmol L^{-1}*

Table 1. Compared with other methods for Cl^- detection

Method	Range of linear	Limit detection	Sample	References
UV	28 μmol L^{-1}-28 mmol L^{-1}	3.6 μmol L^{-1}	natural water	[6]
UV	1.4-22.4 μmol L^{-1}	0.3 μmol L^{-1}	fuel ethanol	[7]
Chromatography	1.4 μmol L^{-1}-0.42 mmol L^{-1}	0.19 μmol L^{-1}	commercial tablet	[11]
Electrochemical	3.0 μmol L^{-1}-0.1mmol L^{-1}	2.0 μmol L^{-1}	synthetic sweat	[13]
Electrochemical	0.25 μmol L^{-1}-250 mmol L^{-1}	0.16 μmol L^{-1}	sweat and hela cells	[14]
Electrochemical	0.2 mmol L^{-1} to 0.7 mmol L^{-1}	0.1 mmol L^{-1}	sea water	[15]
fluorescence	0-0.5 mmol L^{-1}	19 μmol L^{-1}	artificial sweat	[16]
fluorescence	0.02-0.06 mol L^{-1}	0.025 mol L^{-1}	environment water	[17]
fluorescence	0.5 mmol L^{-1}-0.1 mol L^{-1}	0.06 mmol L^{-1}	environment water	[18]
This paper	8.5-300 μmol L^{-1}	0.1 μmol L^{-1}	synthetic sweat	-

Table 2. Recoveries of Cl^- in water sample with the proposed method (n = 3)

Sample	Measure	Added/(μmol L^{-1})	Found/(μmol L^{-1})	RSD/%	Recovery/%
DanJiang water	-	50.0	48.7	2.7	97.4
		90.0	88.3	3.5	98.1
		130.0	134.7	3.1	103.6

Table 3. Detection and Recoveries of Cl^- in artificial sweat samples (n = 3)

Sample	Measured/(μmol L^{-1})	RSD/%	Added/(μmol L^{-1})	Found/(μmol L^{-1})	RSD/%	Recovery/%
1	19.6	3.1	20.0	38.9	2.3	96.5
2	51.3	2.7	50.0	100.2	2.5	97.8
3	83.8	2.1	80.0	167.6	3.9	104.8

CONCLUSIONS

In conclusion, N-GQDs have been synthesized by a hydrothermal method and further characterized by TEM, XRD, UV–Vis and fluorescence. Meanwhile, N-GQDs have been used as a fluorescent probe for Cl^- detection. When introducing Ag^+ into N-GQDs, the fluorescence quenched, while with the addition of Cl^- into the N-GQDs/Ag^+ solution, the fluorescence intensity was enhanced. The sensor had a linear response to Cl^- in the range of 8.5-300 μmol L^{-1} with a detection limit of 0.1 μmol L^{-1}. Finally, it has been used to determine of Cl^- in artificial sweat and environmental water, the satisfactory results further confirmed its practicability. This work provides a simple and low-cost method for the detection of Cl^-, and expands the application of N-GQDs in environmental safety and food safety.

ACKNOWLEDGEMENTS

This project was supported by the National Natural Science Foundation of China (No. 30970696), the Science and Technology Planning Project of ShaanXi Province (2012KTDZ 02-02) and Science and technology innovation team project of shangluo university (18SCX003).

REFERENCES

1. Winterton, N.; *Green Chem.* **2000**, *2*, 173.
2. Montemor, M. F.; Alves, J. H.; Simoes, A. M.; Fernandes, J. C. S.; Lourenço, Z.; Costa, A. J. S.; Appleton, A. J.; Ferreiraa, M. G. S.; *Cem. Concr. Compos*. **2006,** *28*, 233.
3. Ling, B.; Ouyang, S.; Wang, S.; *Innov. Food Sci. Emerg. Technol.* **2019**, *52*, 158.
4. Zhang, M.; Wang, C. Q.; Zhang, Z. Y.; Ye, J.; Fang, P. P.; *Sens. Actuators, B* **2019**, *299*, 126951.
5. Fakhri, H.; Fishman, K. L.; Ranade, R.; *Constr. Build. Mater*. **2021**, *268*, 121148.
6. Yakoh, A.; Rattanarat, P.; Siangproh, W.; Chailapakul, O.; *Talanta* **2018**, *178*, 134.
7. Lima, M. J. A.; Reis, B. F.; *Talanta* **2019**, *201*, 373.
8. Gajdosechova, Z.; Dutta, M.; López-Linares, F.; Mello, P. A.; Iop G. D.; Flores, E. M. M.; Mester, Z.; Pagliano, E.; *Fuel* **2021**, *285*, 119167.
9. Shen, M.; Tu, M. M.; Zhang, W.; Zou, J. H.; Zhang, M.; Cao, Z.; Zou, B. D.; *J. Clin. Lab. Anal.* **2020**, *34*, 1.
10. Robaina, N. F.; Feiteira, F. N.; Cassella, A. R.; Cassella, R. J.; *J. Chromatogr. A* **2016**, *1458*, 112.
11. Novo, D. L. R.; Pereira, R. M.; Hartwig, C. A.; Santos, C. M. M.; Mesko, M. F.; *Talanta* **2018**, *181*, 440.
12. Bin, Q. Y.; Wang, M.; Wang, L. S.; *Nanotechnology* **2020**, *31*, 125601.
13. Bujes-Garrido, J.; Izquierdo-Bote, D.; Heras, A.; Colina, A.; Arcos-Martínez, M. J.; *Anal. Chim. Acta* **2018**, *1012*, 42.
14. Wan, Y. Q.; Hua, Y.; Liu, M.; Li, S.; Yin, M. Y.; Lv, X. X.; Wang, H.; *Sens. Actuators, B* **2019**, *300*, 127058.
15. Bujes-Garrido, J.; Arcos-Martínez, M. J.; *Sens. Actuators, B* **2017**, *240*, 224.
16. Kim, J.; Lee, S.; Kim, S.; Jung, M.; Lee, H.; Han, M. S.; *Dyes Pigm.* **2020**, *177*, 108291.
17. Xiao, W.; Ding, L. Y.; He, J. Y.; Huang, J.; *Opt. Mater*. **2019**, *98*, 109467.
18. Zhang, Z. S.; Gao, Y.; Li, P.; Qu, B. H.; Mu, Z. Y.; Liu, Y.; Qu, Y.; Kong, D. G.; Chang, Q.; Jing, L. Q.; *Chin. Chem. Lett*. **2020**, *31*, 2725.
19. Zhang, F. Y.; Ma, C.; Wang, Y. Y.; Liu, W.; Liu, X. Y.; Zhang, H. X.; *Spectrochim. Acta A* **2018**, *205*, 428.
20. Tian, P.; Tang, L.; Teng, K. S.; Lau, S. P.; *Mater. Today Chem*. **2018**, *10*, 221.
21. Su, D. D.; Wang, M. K.; Liu, Q.; Chen, J. Y.; Su, X. G.; *Sens. Actuators, B* **2019**, 290: 163.
22. Bian, S.; Shen, C.; Qian, Y.; Liu, J.; Xi, F.; Dong, X.; *Sens. Actuators, B* **2017**, *242*, 231.
23. Li, S.; Li, Y.; Cao, J.; Zhu, J.; Fan, L.; Li, X.; *Anal Chem.* **2014**, *86*, 10210.
24. Liu, X. T.; Na, W. D.; Liu, Q.; Su, X. G.; *Anal. Chim. Acta* **2018**, *1028*, 45.
25. Nair, R. V.; Thomas, R. T.; Mohamed, A. P.; Pillai, S.; *Microchem. J.* **2020**, *157*, 104971.
26. Ge, S. Y.; He, J. B.; Ma, C. X.; Liu, J. Y.; Xi, F. G.; Dong, X. P.; *Talanta* **2019**, *199*, 581.
27. Guo, Z. S.; Wu, H.; Li, M.; Tang, T.; Wen, J. F.; Li, X. Y.; *Appl. Surf. Sci.* **2020**, *526*, 146724.
28. Chen, S. F.; Chen, X. Q.; Xia, T. T.; Ma Q.; *Biosens. Bioelectron.* **2016**, *85*, 903.
29. Ozyurt, D.; Shafqat, S; Pakkanen, T. T.; Hocking, R. K.; Mouritz, A.; Fox, B.; *Carbon* **2021**, *175*, 576.
30. Liu, Y., Liu, C. Y.; Liu, Y.; *Appl. Surf. Sci.* **2011**, *257*, 5513.
31. Qu, D.; Zheng, M.; Du, P.; Zhou, Y.; Zhang, L. G.; Li, D.; Tan, H. Q.; Zhao, Z.; Xie, Z. G.; Sun, Z. C.; *Nanoscale* **2013**, *5*, 12272.